Tribology and Materials
Vol. 4, No. 2, 2025, pp. 66-77

ISSN 2812-9717
https://doi.org/10.46793/tribomat.2025.006

Effect of amino-functionalized MWCNTs addition on mechanical and tribological behaviour of polypropylene-based nanocomposites

Durga Prasad MULAGA, Ambuj SHARMA*

School of Mechanical Engineering, VIT-AP University, Amaravati, India
*Corresponding author: sharma.ambuj@vitap.ac.in

Keywords
polypropylene
AMWCNTs
mechanical properties
wear
friction

History
Received: 21-11-2024
Revised: 17-03-2025
Accepted: 18-03-2025

Abstract

Although polypropylene (PP) is lightweight and offers excellent chemical resistance, it shows poor mechanical characteristics for structural applications without reinforcement due to its semi-crystalline structure. This research investigates the mechanical and tribological performance of a polypropylene matrix, incorporating a PP-G-MA compatibilizer and reinforced with both pristine multi-walled carbon nanotubes (MWCNTs) and amino-functionalized multi-walled carbon nanotubes (AMWCNTs) at a weight percentage of 1 wt. %. We made PP/MWCNTs nanocomposite using ultrasonication and magnetic stirring to control the poor dispersion of MWCNTs within the polypropylene matrix, which results in consistent mechanical properties. The performance of the fabricated PP/MWCNTs nanocomposite was compared to that of PP/AMWCNTs using microscopic, mechanical and tribological characterisation techniques. Characterisation was carried out using FTIR spectroscopy to identify functional groups and chemical bonding in the PP matrix, XRD for crystallographic structure and SEM for morphology. Tensile and hardness tests were used to check the materials' mechanical properties, such as their modulus of elasticity, tensile strength and hardness. The tribological characteristics were evaluated using a pin-on-disc tribometer in dry sliding conditions, allowing the assessment of material wear resistance and coefficient of friction. A PP-based nanocomposite reinforced with AMWCNTs exhibits exceptional tensile strength, modulus of elasticity, hardness and wear resistance. This nanocomposite exhibits a 36 % increase in tensile strength and an 87 % increase in wear resistance compared to the pure PP sample. The consistent dispersion of AMWCNTs throughout the matrix and the improved bonding between the AMWCNTs reinforcement and the PP matrix result in the PP/AMWCNTs nanocomposite exhibiting exceptional properties.

1. Introduction

The physical properties, mechanical performance and manufacturing simplicity of polypropylene (PP) make it an ideal engineering plastic [1]. However, it is not very useful because it cracks easily at low temperatures. Scientists address this issue by incorporating carbon-based reinforcements or rubber particles into the PP matrix. Materials are strengthened and made tougher by adding these reinforcements, especially carbon nanotubes (CNTs), graphene or reduced graphene oxide [2,3]. The CNTs are used as reinforcement in polymer matrices due to their large surface area, low density and exceptional thermal, chemical and mechanical capabilities [4-6]. Numerous studies have demonstrated that multi-walled carbon nanotubes (MWCNTs) enhance mechanical performance, electrical conductivity, heat resistance and crystallisation in PP/MWCNTs nanocomposites [7-10].

The thermal conductivity of PP-based nanocomposites was enhanced by adding MWCNTs,

leading to improved heat dissipation in electronic devices [11]. Carbon-based nanofillers in PP-based nanocomposites can boost electronic devices' electromagnetic conductivity, improving their performance. Such improvements can result in more effectiveness in a range of applications, including automobile components and consumer electronics [12]. Nevertheless, an excessive quantity of MWCNTs might negatively impact the mechanical characteristics of the PP-based nanocomposite.

Material scientists have been studying the feasibility of PP-based nanocomposites reinforced with MWCNTs [13-15]. Determining the effect of filler concentration on PP-based nanocomposite characteristics is an important research topic [16-18]. Andrews et al. [19] observed a decrease in strength with high filler amounts, while Liu and Gao [20] found improvements with lower percentages. Bao and Tjong [21] suggest an optimal filler amount for specific applications based on the desired mechanical properties. Stanciu et al. [22] discovered that adding MWCNTs to PP produces nanocomposites with altered characteristics, some of which are useful, such as enhanced tensile strength and modulus of elasticity. Beyond mechanical enhancements, MWCNTs can also improve the fire resistance of PP-based nanocomposites. Zhang et al. [23] and Liu et al. [24] achieved remarkable results with Nylon 6, a compatible polar polymer. Their simple melt compounding method created strong interfaces and well-dispersed nanotubes, leading to significantly stronger nanocomposites. However, Tang et al. [25] and Bhattacharyya et al. [26] were unable to reproduce this achievement when employing nonpolar polyolefins such as high-density polyethylene and polypropylene.

The incompatibility between nonpolar polymers and the nanotubes resulted in poor dispersion and minimal improvement in the final material's properties. Patti et al. [27] highlight the crucial role of compatibility between the polymer matrix and the nanofillers for achieving well-dispersed and effective reinforcements in nanocomposites. Various mixing techniques, such as solution blending and melt mixing, are used to incorporate MWCNTs into PP. Dondero and Gorga [13] focused on achieving good dispersion and orientation of MWCNTs within the PP matrix. Their efforts resulted in a significant improvement in toughness, with a 32 % increase observed for a nanocomposite containing just 0.25 wt. % MWCNTs compared to pure PP. They established that MWCNTs can improve the mechanical properties of PP-based nanocomposites, but appropriate dispersion is crucial for good results.

Carbon-based reinforcements have significantly contributed to the remarkable decreases in the wear rate of the polymer matrix at low loadings. Within the literature, findings differ significantly from one study to another, often influenced by only minor alterations in the reinforcement material or blending methodology. Patel et al. [28] found that 0.5 wt. % of MWCNTs-reinforced PMMA nanocomposites' enhanced tribological performance may be attributed to the effective transmission of load between the MWCNTs and the PMMA matrix, as well as the reinforcing effect of the MWCNTs. The sliding wear of a PP-based nanocomposite reinforced with carbon nanotubes was carried out by Ashok Gandhi et al. [29] on a pin-on-disc tribometer with a steel disc surface under dry conditions. The test was evaluated as a function of the applied load and sliding speed with different amounts of CNTs in PP. The findings demonstrated that an increase in CNTs content enhances wear resistance. On the other hand, Johnney Mertens and Senthilvelan [30] developed PP/CNTs nanocomposites using melt intercalation and conducted wear tests under dry sliding conditions. The observation made during the ploughing process indicated that the self-lubricated characteristic of CNTs did not exert any effect or influence throughout the experiment. The wear resistance of the PP-based nanocomposite is inferior to that of the pure PP samples.

Despite the significant progress in PP/MWCNTs nanocomposites, there are still challenges to address. These challenges include the nonhomogeneous dispersion of MWCNTs reinforcement in the PP matrix and the agglomeration of reinforcements. To overcome these issues, researchers are controlling the dimensions of the PP molecules, implementing post-mixing treatments and employing additives to improve the mixing process. However, further research is necessary to meet the criteria of structural applications. The literature review indicates that many studies have been conducted to explore the tribological characteristics of polymeric nanocomposites. However, limited research has documented the wear performance of PP-based nanocomposites reinforced with modified MWCNTs under dry sliding conditions.

The main purpose of this study is to compare the effects of amino-functionalized MWCNTs (AMWCNTs) and non-functionalized MWCNTs

reinforcement on the mechanical and tribological properties of PP-based nanocomposites. Previous research has shown that a low amount of MWCNTs (≤ 1 wt. %) effectively improves wear resistance, hardness and load-bearing capacity while preventing the problems with processing that come up with higher concentrations of MWCNTs [31]. The 1 wt. % AMWCNTs was specifically selected to address the dispersion limitations of non-functionalized MWCNTs. Amino functional groups improve compatibility with the PP matrix, reducing agglomeration and enhancing stress transfer. The present study also aimed to enhance the homogenisation of MWCNTs in PP. The first step in this approach involved the attachment of PP with tiny molecules that have chemical groups, namely maleic anhydride (PP-G-MA). Furthermore, the MWCNTs are altered to include amino groups (MWCNTs-NH_2) on their surface. The combination of PP-G-MA and MWCNTs-NH_2 facilitated the chemical bonding of PP chains to the MWCNTs. This process led to the creation of a PP/PP-G-MA/amino-functionalized MWCNTs nanocomposite. This method enhanced the dispersion of MWCNTs within the PP, resulting in durable and more thermally resistant composite products.

2. Materials and methods

2.1 Materials

This investigation employed the Repol H110MA PP resin from Reliance Industries, India. The PP resin density was 0.910 g/cm^3, and the melt flow rate was 11 g/10 min at 230 °C under a load of 2.16 kg. The polypropylene grafted maleic anhydride (PP-G-MA) copolymer, with a melt flow rate of 15 g/10 min at 2.16 kg and 230 °C, obtained from Plus Polymer, India, was used as a compatibilizer in the fabrication of the nanocomposites. The MWCNTs, supplied by AD Nano Technologies, India, had an average length of 10 – 50 nm, an average diameter of 10 – 30 nm and a purity of more than 95 – 99 vol. %. The (3-Aminopropyl)triethoxysilane (APTES) was used to improve the bonding of the polymer to the MWCNTs. APTES, with a molecular weight of 179.29 g/mol and a density of 1.027 g/cm^3, improved the polymer's morphological properties, resulting in more uniformly dispersed particles.

2.2 Fabrication of nanocomposites

Two PP matrix nanocomposites were produced: one reinforced with pristine (non-functionalized) MWCNTs and the other with amino-functionalized MWCNTs. This study employed the same steps to investigate the effects of amino-functionalized and non-functionalized MWCNTs on the properties of the PP-based nanocomposites. The PP-G-MA was incorporated into the non-functionalized MWCNTs to improve the interfacial adhesion between the PP matrix and the MWCNTs. The surface of non-functionalized MWCNTs is hydrophobic, and they do not mix well with the nonpolar PP matrix. This makes it hard for the nanoparticles to spread out and forms weak bonds between them.

The nanocomposites were processed using a twin screw extruder 25TS/CO/300/30 at 210 °C and 80 rpm (Aasabi Machinery). The PP-G-MA compatibilizer was incorporated to improve the material properties. The composite melt was then extruded into a continuous wire, quenched in a water bath and pelletized. To minimise void formation and moisture-induced degradation, both the PP-G-MA compatibilizer and the pure PP containing nanofillers were dried in a vacuum oven at 80 °C for four hours before melting. The pelletized nanocomposites were then injection moulded into standard test specimens using a semiautomatic machine IM-D30 (Deesha Impex) under the following conditions: a melt temperature of 200 – 215 °C, a mould temperature of 25 °C, a holding pressure of 6 MPa and an injection speed of 100 rpm. The extruded wire was passed through a water basin at room temperature for rapid cooling (quenching), after which the material was cut and pelletized for further use. For the fabrication of test specimens, the pellets were injected into a die cavity under a pressure of 1 MPa, with the temperature of the injection moulding die maintained at 230 °C. The specimens were prepared per ASTM D638, Type IV. The pure PP and PP-based nanocomposite pellets were vacuum-dried at 80 °C before being used to ensure their optimal properties. The final polymer-based nanocomposites contained 1 wt. % of either MWCNTs or AMWCNTs. For comparative analysis, we processed pure PP using the same extrusion and injection moulding steps, which served as a control for mechanical and tribological property evaluations. Figure 1 illustrates the steps involved in the complete PP/MWCNTs sample fabrication process. The detailed composition of fabricated samples and their designations are given in Table 1. The manuscript refers to the pure PP sample as S1, the non-functionalized MWCNTs sample as S2 and the amino-functionalized MWCNTs sample as S3.

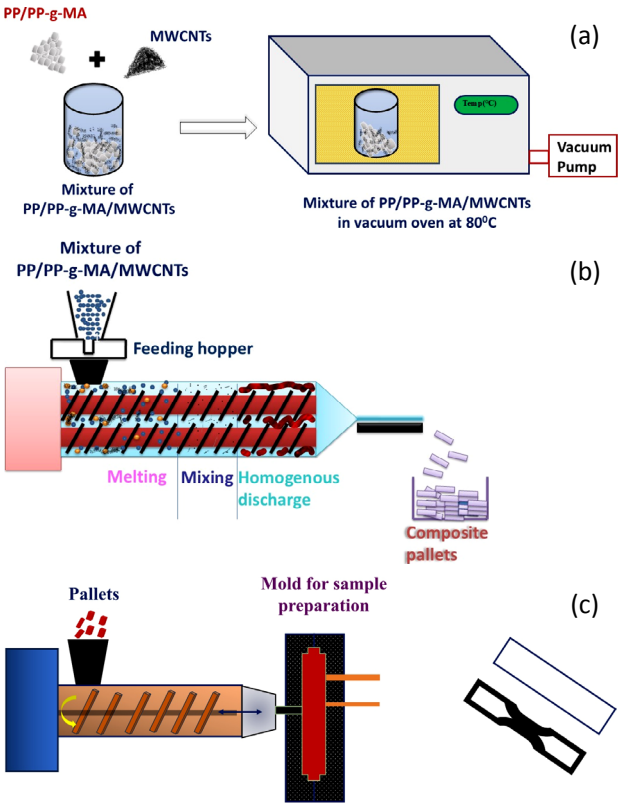

Figure 1. Fabrication process of PP/MWCNTs sample: (a) mixing of PP/PP-G-MA/MWCNTs followed by vacuum oven treatment, (b) PP/PP-G-MA/MWCNTs mixture poured in twin screw extruder and (c) sample prepared by injection moulding

Table 1. Designation and composition details of nanocomposites

Designation	Composition	
	nominal	wt. %
S1	PP	100
S2	PP/PP-G-MA/MWCNTs	96/3/1
S3	PP/PP-G-MA/AMWCNTs	96/3/1

2.3 Characterisation of nanocomposites

PP and PP-based nanocomposites were analysed using Fourier transform infrared spectroscopy (FTIR) and X-ray diffraction (XRD). FTIR spectra were recorded with a Cary 630 FTIR spectrometer (Agilent Technologies), covering a wavenumber range of 400 – 4000 cm^{-1}. XRD patterns were obtained using a Cu Kα radiation source (λ = 1.54 Å) on a Rigaku MiniFlex diffractometer, with a scanning range from 5 to 90°. Injection moulded nanocomposite samples were used for scanning electron microscopy (SEM). To see the internal morphology of the PP-based nanocomposites, the samples were cryogenically fractured by immersing them in liquid nitrogen for 150 to 200 seconds. This dwell period ensures that the polymer matrix becomes sufficiently brittle, preventing plastic deformation during fracture. A Carl Zeiss EVO 10 SEM, operating at 5 kV in a high vacuum, was used for microstructural analysis.

The mechanical strengths of all fabricated nanocomposites were evaluated using tensile testing. Tensile strength and modulus of elasticity were determined according to ASTM D638 using a Tinius Olsen H10KL universal testing machine. The tests were conducted at room temperature with a feed rate of 1 mm/min. The stress-strain curves obtained were analysed to calculate the mechanical properties. The reported tensile strength and modulus of elasticity values for each material are the averages of five individual specimen tests. Microhardness measurements were conducted using a Chennai Metco VH-1MDX Vickers hardness tester with a diamond indenter. The tests were performed at a load of 0.05 kg (0.49 N) to assess the hardness variation across the samples. The average hardness values were determined by taking the mean of five individual measurements from each test specimen.

The tribological properties of pure PP and PP-based nanocomposites were evaluated using a Ducom TR-20LE pin-on-disc tribometer. The counter-body was a hardened ground steel EN31 disc. The disc had a diameter of 165 mm, a thickness of 8 mm and a hardness of 62 HRC. The surface roughness was *Ra* = 0.6 µm. A normal load of 40 N was used for the tribological tests, equivalent to 0.4 MPa of contact pressure. This created realistic stress conditions for studying the tribological behaviour of PP and PP-based nanocomposite samples. A sliding speed of 0.837 m/s was maintained to simulate moderate wear conditions, balancing thermal effects and material removal rates. The total sliding distance of 3016 m is long enough to assess the progressive wear mechanisms. Square-shaped specimens, each measuring 10 × 10 mm with a thickness of 4 mm, were prepared through injection moulding. These specimens were securely attached to a rectangular holder with adhesive. The tribological tests were repeated three times for each sample (S1, S2 and S3) to ensure the reliability and consistency of the results. Throughout the testing process, wear and friction were continuously measured to monitor real-time variations in tribological performance. All experiments were conducted at a constant room temperature of 24 °C.

3. Results and discussion

3.1 FTIR and XRD characterisation

Adding PP-G-MA to PP along with AMWCNTs increases the compatibility between the nanotube filler and the polymer matrix. Figure 2 illustrates the use of FTIR spectroscopy to analyse the interaction between AMWCNTs and PP-G-MA, confirming this enhanced compatibility. The FTIR spectra of the pure PP matrix (S1), PP with MWCNTs (S2) and PP with AMWCNTs (S3) were compared. The appearance of a new peak at 1670 cm^{-1} in the FTIR spectrum of the PP/MWCNTs and PP/AMWCNTs nanocomposites indicates the formation of imide bonds. This indicates a chemical reaction between the amino groups on the AMWCNTs and the anhydride groups in PP-G-MA. The nanocomposite spectra displayed several prominent peaks. A broad peak centred around 2902 cm^{-1} is attributed to C-H stretching vibrations, while bands at approximately 1235 cm^{-1} correspond to C-H bending modes [32]. Less intense peaks at 1390 cm^{-1} are associated with symmetric C-C ring stretching. Notably, the peak width-to-intensity ratio gradually decreased in the PP/AMWCNTs compared to the PP/MWCNTs, indicating evolving molecular interactions and structural changes within the nanocomposites. The broader peaks in the PP/MWCNTs (S2) sample suggest a more amorphous structure or a more complex distribution of molecular environments, whereas the narrower peaks in the PP/AMWCNTs (S3) sample suggest increased order or regularity in the molecular structure. The introduction of amino (NH_2) groups could potentially influence polymer chain packing and interactions with MWCNTs.

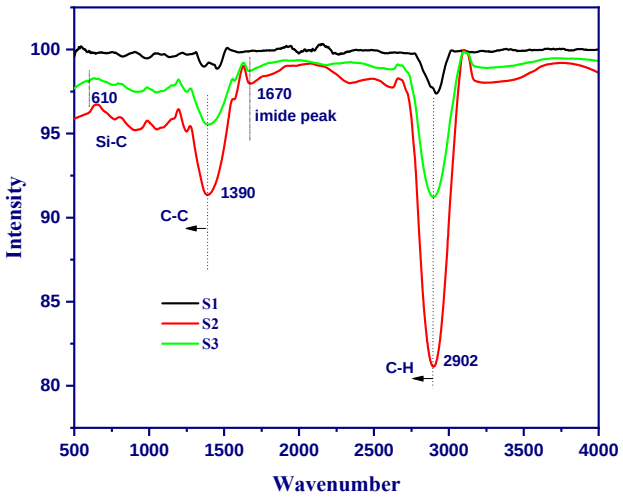

Figure 2. FTIR spectra of PP and PP-based nanocomposites

The XRD is used to look at the crystalline structure of pure PP matrix, PP/MWCNTs and PP/AMWCNTs nanocomposites, which can be seen in Figure 3. For pure PP, the XRD patterns revealed many diffraction peaks. These peaks corresponded to different crystallographic planes of the α phase, such as (110), (040), (130), (131) and (060) at 2θ angles of 13.87, 16.67, 18.26, 21.5 and 25.22°, respectively. It is well established that PP can exist in two crystalline forms: α and β. The significantly higher intensity of the (040) peak compared to the (110) peak for the pure PP matrix indicates a predominant α-phase growth along the (040) plane, confirming that the PP phase present in all samples is the α phase [33,34]. This is the most common and stable crystalline form of PP. To quantitatively assess the evolution of the crystal structure, the ratio of the (040) to (110) peak intensities (I040/I110) is calculated, which yielded a value of 1.3 for pure PP.

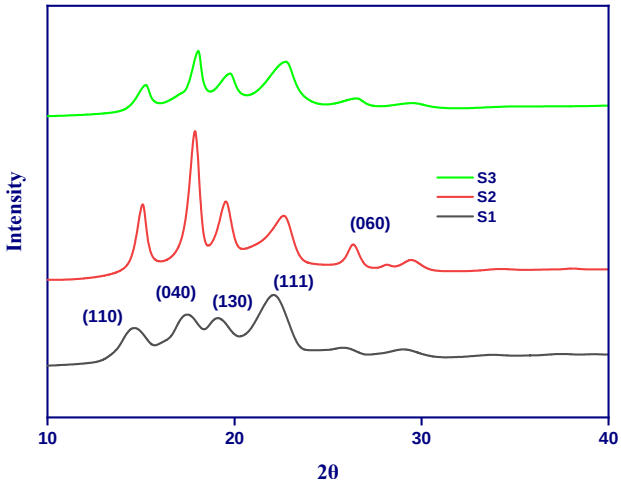

Figure 3. XRD spectra of PP and PP-based nanocomposites

Introducing MWCNTs into the PP matrix also led to the formation of the α phase. However, the peak intensities ratio I040/I110 increased from 1.3 to 1.6 for PP/MWCNTs nanocomposite, indicating faster crystal growth along the (040) plane compared to pure PP. This indicates that MWCNTs influence the crystal structure of the PP. The XRD patterns for PP/AMWCNTs nanocomposite showed only the α phase of PP, with no evidence of the β phase. The β phase in PP forms only in the presence of specific β-nucleating agents or nanoparticles [35]. This study did not use agents like quinacridone derivatives, pimelic acid salts or rare earth compounds [36]. Without them, PP typically crystallises into the more stable α phase.

Additionally, the cooling rate and processing temperature influence the crystalline structure. Since these conditions were not optimised for β phase formation, the α phase is more likely to form. Notably, the I040/I110 ratio for this nanocomposite was the lowest at 1.1, depicting that the (040) and (110) planes contributed almost equally to crystal growth. This means that AMWCNTs more effectively promote a uniform crystal orientation in the PP matrix than MWCNTs. Furthermore, a slight shift in peak positions was noticed between the PP/AMWCNTs and PP/MWCNTs nanocomposite. This subtle shift suggests that the incorporation of functional groups onto the MWCNTs surface has a minor effect on the crystallographic parameters of the PP phase. This result suggests that the AMWCNTs and PP chains may interact with each other, which may slightly alter the packing and arrangement of the polymer chains within the crystal lattice.

3.2 Mechanical properties

Figure 4 displays a tensile stress-strain graph for the PP matrix and MWCNTs/AMWCNTs nanocomposites. Figure 5 represents the calculated value of the tensile strengths, and Figure 6 summarises the modulus of elasticity values. The PP matrix (S1) had a modulus of elasticity of 2.4 GPa and a tensile strength of 35.8 MPa. Incorporating non-functionalized MWCNTs into the PP matrix (S2) resulted in modest improvements, increasing the modulus of elasticity by 34 % and tensile strength by 20 %. The tensile properties of the sample S2 improved due to the effective dispersion of MWCNTs within the PP matrix [9], as confirmed by XRD analysis. Fine fibrils and microvoids formed in the stress-whitening region further supported these enhanced properties. PP/AMWCNTs nanocomposite (S3) showed the most significant improvements, with a 53 % modulus of elasticity and a 36 % tensile strength increase. Covalent bonding between the PP chains and MWCNTs enhanced load transfer from the matrix to the nanotubes. During tensile testing, all materials exhibited visible stress-whitening. This enhancement can be attributed to the reactive compatibilization between AMWCNTs and PP-G-MA (as confirmed by FTIR spectroscopy in Figure 2), the finer dispersion of AMWCNTs within the PP matrix and the increased crystallinity of the nanocomposite.

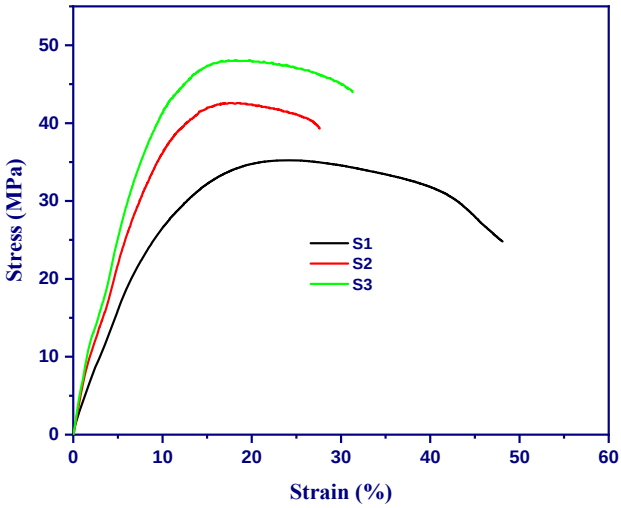

Figure 4. Stress-strain curves of PP and PP-based nanocomposites

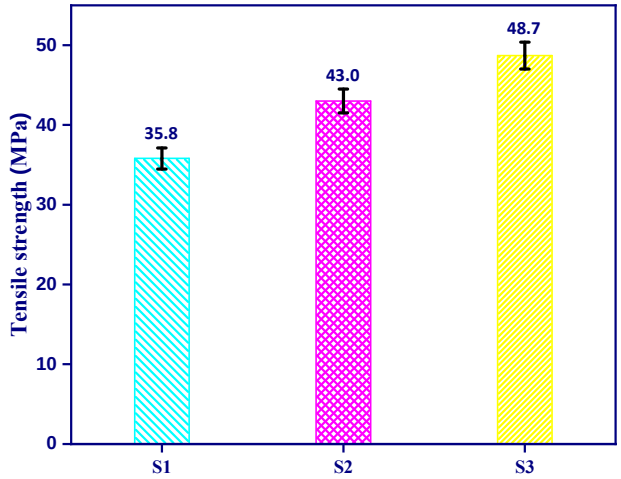

Figure 5. Tensile strengths of PP and PP-based nanocomposites

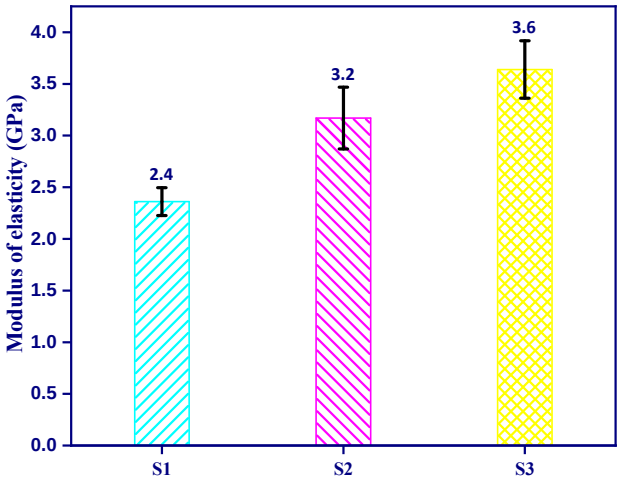

Figure 6. Modulus of elasticity of PP and PP-based nanocomposites

Figure 7 presents the average hardness values for PP and PP-based nanocomposites. The hardness of sample S1 is 1.4 HV 0.05, but it goes up to 5.2 HV 0.05 in sample S2 because of the MWCNTs'

reinforcement effect. The hardness further improves in sample S3, reaching 8 HV 0.05, representing the highest value among all tested samples. The increase in hardness seen from S1 to S2 is due to the high strength and stiffness of MWCNTs, which strengthen the PP matrix because of their high length-to-diameter ratio. The further enhancement in S3 is primarily due to the amino-functionalization of MWCNTs, which significantly improves interfacial adhesion with the matrix. This stronger interfacial interaction leads to better dispersion of MWCNTs within the matrix, significantly improving the nanocomposite's hardness.

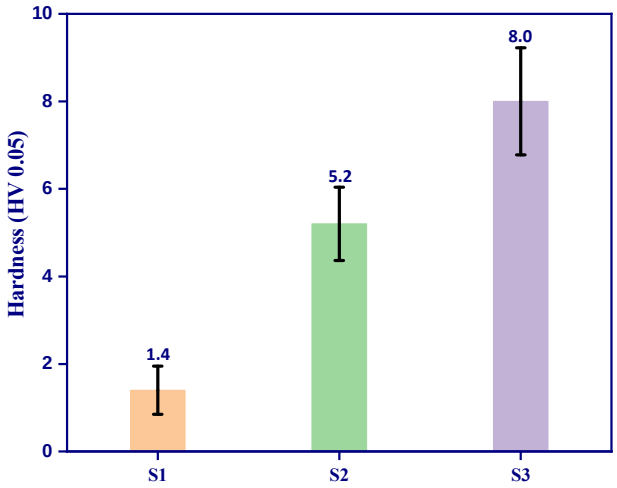

Figure 7. Hardness of PP and PP-based nanocomposites

3.3 Cryogenic fracture morphology

Figure 8 displays SEM images of the fracture surfaces of test specimens. Microstructure analysis of the PP matrix revealed shear band formation, as seen in Figure 8a. Figure 8b shows that PP/MWCNTs nanocomposite formed microvoids in the stress-whitening region. The SEM image of the S2 sample also reveals poor dispersion of MWCNTs, which is characterised by large MWCNTs agglomerates and numerous unbroken nanotubes visible on the fracture surface. These agglomerates act as stress concentrators, leading to premature failure due to ineffective load transfer. To highlight these microstructural features, MWCNTs agglomeration is marked with a yellow rectangle, while poor MWCNTs dispersion is indicated using a yellow ellipse. Microvoids, which contribute to the stress-whitening effect and fracture propagation, are highlighted by a yellow triangle. The presence of these defects suggests that inadequate dispersion of MWCNTs can limit reinforcement efficiency. This can result in an early failure under tensile stress.

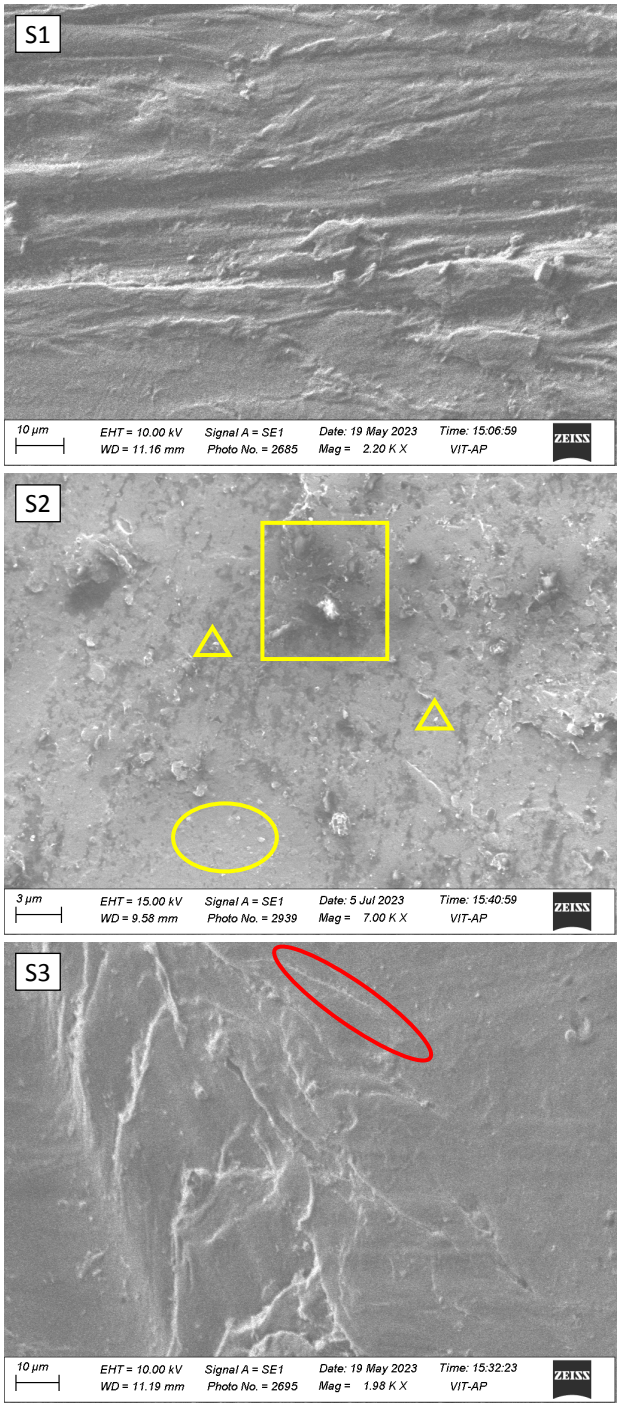

Figure 8. SEM images of cryogenically fractured samples

Figure 8c presents the fracture surface morphology of the PP/AMWCNTs nanocomposite. A more uniform dispersion of MWCNTs within the matrix is noticed compared to the non-functionalized MWCNTs. The better distribution and less clustering of AMWCNTs show that the nanotubes and matrix have strong interfacial adhesion, which improves the mechanical performance. The finer fibrillar structure noticed in PP/AMWCNTs indicates that amino-functionalized MWCNTs (AMWCNTs) are better integrated into

the PP matrix. This results in improved stress transfer during mechanical loading. The presence of amino-functionalization around PP fibrils is highlighted by a red-coloured ellipse, emphasising the improved interaction at the interface. In S2 and S3 samples, the addition of compatibilizers effectively reduced aggregate size and enhanced MWCNTs dispersion. This indicates that PP-G-MA compatibilizers improved MWCNTs dispersion by decreasing interfacial tension between the PP matrix and nanotubes [37].

3.4 Tribological behaviour

Common wear mechanisms for polymers and their composites include abrasion, adhesion and fatigue. Pin-on-disc tests were performed on pure PP and PP-based nanocomposites to investigate the lubricating effect of amino-functionalized and non-functionalized MWCNTs.

Figure 9 represents the coefficient of friction (COF) versus time for PP and PP-based nanocomposites. The COF of the PP-based nanocomposites (S2 and S3) is lower than the PP (S1) due to the weak van der Waals forces between the MWCNTs and PP matrix. The average PP COF value in the steady-state zone, from 900 to 1500 s, is 0.71 ± 0.02. The average COF of sample S2 is 0.46 ± 0.01, from 600 to 852 s, whereas COF for sample S3 is 0.57 ± 0.02, from 1200 to 1600 s. In the initial stage of sliding, from 0 to 100 s, PP shows a relatively high COF, primarily due to its inherent surface roughness and adhesion between the contacting surfaces (polymer and steel disc). As wear progresses, from 100 to 600 s, localised softening of the polymer matrix may occur, and temporarily unstable friction can be noticed. After 900 s, the COF tends to stabilise and increase, which can be attributed to plastic deformation of the surface and enhanced adhesion and abrasion. The intermediate zone, from 900 to 1500 s, can be considered a steady-state zone where COF stabilises and slightly increases. In extended sliding time, from 2400 to 3600 s, the COF remains elevated or increases further due to progressive material degradation. Abrasion and fatigue cause fluctuations in friction in this zone [38].

Sample S2 showed lower COF than samples S1 and S3. During the initial stage of sliding, from 0 to 520 s, the COF decreased. This decrease is primarily due to the MWCNTs reinforcement in the PP matrix, which prevents direct polymer-to-polymer contact and makes the structure more rigid. However, due to the poor dispersion of non-functionalized MWCNTs in the PP matrix, the COF value in sample S2 fluctuates more over time compared to sample S3. This shows that the load is not evenly distributed and that there are areas of high stress. As the wear process progresses, from 520 to 970 s, wear debris generated from the polymer matrix and nanotube detachment may act as a temporary lubricant, leading to friction stabilisation [29]. After 970 s, the weak interfacial adhesion between non-functionalized MWCNTs and the PP matrix results in gradual nanotube pullout, which can cause fluctuation and localised increases in COF.

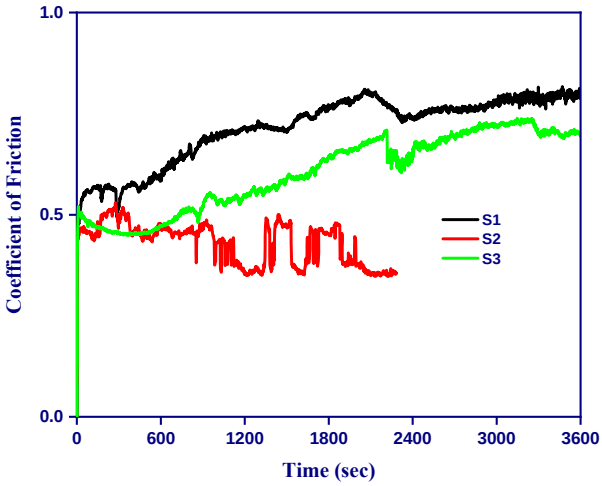

Figure 9. COF of PP and PP-based nanocomposites vs. time

Sample S3 demonstrated the lowest COF during the initial stage of sliding, which lasted from 0 to 520 s. This decrease in friction is primarily due to the better mixing of amino-functionalized MWCNTs into the polymer matrix and their stronger bonding with PP at the interface. Additionally, amino-functionalized MWCNTs act as solid lubricants, minimising further friction at the contact interface. As the test progresses to the intermediate stage, up to 2215 s, the COF stays stable because the functionalized nanotubes stick firmly to the PP matrix. This prevents the nanotubes from separating and ensures effective load transfer. Over an extended period, from 2300 to 3600 s, sample S3 maintained a stable COF.

Figure 10 shows the wear (material thickness loss) in micrometres versus time for PP and PP-based nanocomposites. Pure PP shows the highest wear as compared to non-functionalized and amino-functionalized MWCNTs-reinforced nanocomposites. PP is a semi-crystalline thermoplastic with low hardness and a relatively

low melting temperature, leading to the highest wear. For the first 350 s of sliding, the wear is negative (−35 µm) due to material transfer to the steel disc and localised plastic deformation rather than immediate material removal. Between 350 and 495 s, wear stabilises. After 495 s, intensive wear is noticed in PP due to repeated frictional heating that softens the matrix and causes localised thermal degradation. Poor mechanical properties of PP, which have been previously highlighted, contribute to the increase of material removal. Within the steady-state zone, between 1235 and 2000 s, wear is measured as 2012 ± 5.3 µm. Progressively increasing wear can be noticed after 2400 and up to 3600 s due to fatigue wear and plastic deformation.

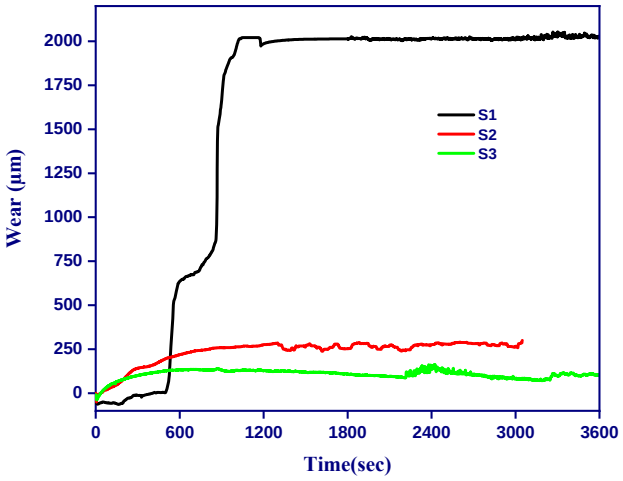

Figure 10. Wear of PP and PP-based nanocomposites vs. time

As shown in Figure 10, the non-functionalized MWCNTs-reinforced PP matrix has higher wear resistance than sample S1 but lower wear resistance than sample S3. The presence of MWCNTs as reinforcement in the PP matrix increases mechanical properties, such as stiffness and hardness. This improvement helps to lower the wear compared to sample S1. Furthermore, minimising polymer-to-polymer friction is another reason for lower wear. For the first 300 s of sliding, wear was intensive due to localised plastic deformation. Thereafter, wear increased gradually until 600 s. Between 600 and 1200 s, wear was stable and considered as steady-state wear. In the steady-state zone, the average wear was 256 ± 2 µm. The gradual pullout of nanotubes from the matrix during sliding causes a fluctuation in wear after 1300 s of sliding. The wear increased after 2400 s due to both abrasive and adhesive wear. MWCNTs pullout contributes further to material degradation. However, the wear is lower than that of PP, but it remains inconsistent due to agglomeration and poor dispersion of MWCNTs in the PP matrix, which was previously noticed.

The amino-functionalized MWCNTs-reinforced PP-based nanocomposite (S3) is more wear resistant than samples S1 and S2. This significant reduction in wear of sample S3 is due to better dispersion and stronger interfacial bonding between the MWCNTs and the PP matrix. For the first 125 s of sliding, the wear is intensive. Thereafter, from 125 to 440 s, it gradually increases but stays lower compared to sample S2. Between 440 and 2100 s, wear is very stable and may be considered as steady-state wear. The average wear in this zone was 122 ± 10 µm, which is the lowest among the samples. This stability in wear over time comes from uniform dispersion of MWCNTs and improved adhesion with the matrix. This process enables efficient load transfer and restricts matrix deformation. Furthermore, there is a fluctuation in wear, from 2200 to 2600 s, because nanotubes are pulled out, which causes the PP matrix to deform in some places. Between 2600 and 3200 s, wear stabilises with more fluctuations due to wear debris. Thereafter, fatigue wear can be noticed. Amino-functionalized MWCNTs act as nanoscale lubricants, mitigating wear-induced heat. This process keeps the structure stable over time and lowers the wear.

Samples S2 and S3 had significantly reduced wear and friction compared to sample S1. Specifically, the wear decreased by 73 % for S2 and by 87 % for S3, considering only steady-state zone average values. Regarding COF, the reduction was 40 % for S2 and 19 % for S3 compared to pure PP. Both nanocomposites show lower friction than PP, but S2 shows a more intensive decrease. The wear rate of PP was calculated as 0.0014 mm^3/m, indicating significant wear under dry sliding conditions. When 1 wt. % non-functionalized MWCNTs were added, the wear rate decreased to 0.00071 mm^3/m. This material showed a moderate improvement in wear resistance, but it was limited by poor dispersion and weak interfacial bonding, which can cause MWCNTs to pullout. The amino-functionalized MWCNTs-reinforced PP-based nanocomposite had an even lower wear rate of 0.00054 mm^3/m. The lower wear rate was because the AMWCNTs were spread out more evenly and had stronger interfacial adhesion, which improved load transfer. This makes it more wear resistant while keeping a moderate friction level.

4. Conclusion

This research shows that AMWCNTs-reinforced PP-based nanocomposite has better mechanical and tribological properties than PP/MWCNTs nanocomposite. The results indicate that surface functionalization is key to better nanofiller dispersion, interfacial adhesion and load transfer in the polymer matrix.

FTIR spectroscopy confirmed that imide bonds formed between PP-G-MA and AMWCNTs. These bonds made the interactions between the nanofiller and matrix stronger and increased chemical stability.

XRD analysis indicated that adding AMWCNTs made the crystal orientations more uniform in the PP matrix, which improved the structure's stability and order. A slight change in peak positions between functionalized (PP/AMWCNTs) and non-functionalized (PP/MWCNTs) nanocomposite is also noticed. This variation was due to strong interactions between the AMWCNTs and PP chains.

The covalent bonding between the PP chains and the AMWCNTs surfaces improved the interfacial bonding, increasing mechanical strength and decreasing wear. Cryogenic fracture morphology analysis indicated uniform dispersion of AMWCNTs, which minimised agglomeration and ensured homogeneous reinforcement.

Compared to pure PP, PP/AMWCNTs nanocomposite had a 53 % higher modulus of elasticity and a 36 % higher tensile strength. This improvement was because it was better at transferring stress and having nanofillers reinforce them.

Tribological testing revealed a 73 % reduction in wear for PP/MWCNTs nanocomposite and an 87 % reduction for PP/AMWCNTs nanocomposite compared to pure PP. The coefficient of friction was 40 % lower for the PP/MWCNTs nanocomposite and 19 % lower for the PP/AMWCNTs nanocomposite compared to pure PP. This shows effective load distribution and reduced adhesive wear.

The results suggest that PP/AMWCNTs nanocomposite is a promising material for applications that require high mechanical strength and wear resistance.

References

[1] H. Wu, J. Zhang, C. Zhang, J. Feng, M.A. Rahman, E. Baer, Structure-properties relationship of a novel multilayer film/foam material produced through co-extrusion and orientation, Industrial & Engineering Chemistry Research, Vol. 55, No. 41, 2016, pp. 10947-10954, DOI: 10.1021/acs.iecr.6b03418

[2] D.P. Mulaga, A. Sharma, P. Tambe, Graphene nanoribbons reinforced polymer nanocomposites and its applications: A review, Journal of Physics: Conference Series, Vol. 2225, 2022, Paper 012004, DOI: 10.1088/1742-6596/2225/1/012004

[3] T. Sharika, J. Abraham, M. Arif P, S.C. George, N. Kalarikkal, S. Thomas, Excellent electromagnetic shield derived from MWCNT reinforced NR/PP blend nanocomposites with tailored microstructural properties, Composites Part B: Engineering, Vol. 173, 2019, Paper 106798, DOI: 10.1016/j.compositesb.2019.05.009

[4] M. Sabet, Multi-walled carbon nanotube reinforcement in polypropylene nanocomposites: comprehensive analysis of thermal behavior, mechanical properties, and dispersion characteristics, Journal of Thermal Analysis and Calorimetry, Vol. 149, No. 8, 2024, pp. 3165-3179, DOI: 10.1007/s10973-024-12893-3

[5] I. Marriam, F. Xu, M. Tebyetekerwa, Y. Gao, W. Liu, X. Liu, Y. Qiu, Synergistic effect of CNT films impregnated with CNT modified epoxy solution towards boosted interfacial bonding and functional properties of the composites, Composites Part A: Applied Science and Manufacturing, Vol. 110, 2018, pp. 1-10, DOI: 10.1016/j.compositesa.2018.04.011

[6] D. Liu, P. Yang, H. Zhang, M. Liu, W. Zhang, D. Xua, J. Gao, Direct reductive coupling of nitroarenes and alcohols catalysed by Co-N-C/CNT@AC, Green Chemistry, Vol. 21, No. 8, 2019, pp. 2129-2137, DOI: 10.1039/C8GC03818J

[7] M. Sabet, Enhancing the thermal and crystallization properties of polypropylene through carbon nanotube integration: A comprehensive investigation, Iranian Polymer Journal, Vol. 33, No. 6, 2024, pp. 727-741, DOI: 10.1007/s13726-024-01278-w

[8] V. Eckert, E. Haubold, S. Oswald, S. Michel, C. Bellmann, P. Potapov, D. Wolf, S. Hampel, B. Büchner, M. Mertig, A. Leonhardt, Investigation of the surface properties of different highly aligned N-MWCNT carpets, Carbon, Vol. 141, 2019, pp. 99-106, DOI: 10.1016/j.carbon.2018.09.035

[9] D. Bikiaris, Microstructure and properties of polypropylene/carbon nanotube nanocomposites, Materials, Vol. 3, No. 4, 2010, pp. 2884-2946, DOI: 10.3390/ma3042884

[10] E. Roumeli, D.G. Papageorgiou, V. Tsanaktsis, Z. Terzopoulou, K. Chrissafis, A. Avgeropoulos, D.N. Bikiaris, Amino-functionalized multiwalled carbon nanotubes lead to successful ring-

opening polymerization of poly(ε-caprolactone): Enhanced interfacial bonding and optimized mechanical properties, ACS Applied Materials & Interfaces, Vol. 7, No. 21, 2015, pp. 11683-11694, DOI: 10.1021/acsami.5b03693

[11] S. Sonawane, P. Thakur, R. Paul, Study on thermal property enhancement of MWCNT based polypropylene (PP) nanocomposites, Materials Today: Proceedings, Vol. 27, No. 1, 2020, pp. 550-555, DOI: 10.1016/j.matpr.2019.12.018

[12] A.A. Koval'chuk, V.G. Shevchenko, A.N. Shchegolikhin, P.M. Nedorezova, A.N. Klyamkina, A.M. Aladyshev, Effect of carbon nanotube functionalization on the structural and mechanical properties of polypropylene/MWCNT composites, Macromolecules, Vol. 41, No. 20, 2008, pp. 7536-7542, DOI: 10.1021/ma801599q

[13] W.E. Dondero, R.E. Gorga, Morphological and mechanical properties of carbon nanotube/polymer composites via melt compounding, Journal of Polymer Science Part B: Polymer Physics, Vol. 44, No. 5, 2006, pp. 864-878, DOI: 10.1002/polb.20743

[14] Z. Li, Z. Ying, M. Liu, H.-M. Cheng, Preparation and tensile properties of MWNT/polypropylene composite fibers by melt spinning, New Carbon Materials, Vol. 20, No. 2, 2005, pp. 108-114.

[15] Z. Zhou, S. Wang, Y. Zhang, Y. Zhang, Effect of different carbon fillers on the properties of PP composites: Comparison of carbon black with multiwalled carbon nanotubes, Journal of Applied Polymer Science, Vol. 102, No. 5, 2006, pp. 4823-4830, DOI: 10.1002/app.24722

[16] Z. Spitalsky, D. Tasis, K. Papagelis, C. Galiotis, Carbon nanotube-polymer composites: Chemistry, processing, mechanical and electrical properties, Progress in Polymer Science, Vol. 35, No. 3, 2010, pp. 357-401,DOI: 10.1016/j.progpolymsci.2009.09.003

[17] J.N. Coleman, U. Khan, W.J. Blau, Y.K. Gun'ko, Small but strong: A review of the mechanical properties of carbon nanotube-polymer composites, Carbon, Vol. 44, No. 9, 2006, pp. 1624-1652, DOI: 10.1016/j.carbon.2006.02.038

[18] M.T. Byrne, Y.K. Gun'ko, Recent advances in research on carbon nanotube-polymer composites, Advanced Materials, Vol. 22, No. 15, 2010, pp. 1672-1688, DOI: 10.1002/adma.200901545

[19] R. Andrews, D. Jacques, M. Minot, T. Rantell, Fabrication of carbon multiwall nanotube/polymer composites by shear mixing, Macromolecular Materials and Engineering, Vol. 287, No. 6, 2002, pp. 395-403, DOI: 1439-2054(20020601)287:6<395::AID-MAME395>3.0.CO;2-S

[20] Y.H. Liu, J.L. Gao, Mechanical properties and wear behavior of polypropylene/carbon nanotube nanocomposites, Advanced Materials Research, Vol. 299-300, 2011, pp. 798-801, DOI: 10.4028/www.scientific.net/AMR.299-300.798

[21] S.P. Bao, S.C. Tjong, Mechanical behaviors of polypropylene/carbon nanotube nanocomposites: The effects of loading rate and temperature, Materials Science and Engineering: A, Vol. 485, No. 1-2, 2008, pp. 508-516, DOI: 10.1016/j.msea.2007.08.050

[22] N.-V. Stanciu, F. Stan, I.-L. Sandu, C. Fetecau, A.-M. Turcanu, Thermal, rheological, mechanical, and electrical properties of polypropylene/multi-walled carbon nanotube nanocomposites, Polymers, Vol. 13, No. 2, 2021, Paper 187, DOI: 10.3390/polym13020187

[23] W.D. Zhang, L. Shen, I.Y. Phang, T. Liu, Carbon nanotubes reinforced Nylon-6 composite prepared by simple melt-compounding, Macromolecules, Vol. 37, No. 2, 2004, pp. 256-259, DOI: 10.1021/ma035594f

[24] T. Liu, I.Y. Phang, L. Shen, S.Y. Chow, W.-D. Zhang, Morphology and mechanical properties of multiwalled carbon nanotubes reinforced Nylon-6 composites, Macromolecules, Vol. 37, No. 19, 2004, pp. 7214-7222, DOI: 10.1021/ma049132t

[25] W. Tang, M.H. Santare, S.G. Advani, Melt processing and mechanical property characterization of multi-walled carbon nanotube/high density polyethylene (MWNT/HDPE) composite films, Carbon, Vol. 41, No. 14, 2003, pp. 2779-2785, DOI: 10.1016/S0008-6223(03)00387-7

[26] A.R. Bhattacharyya, T.V. Sreekumar, T. Liu, S. Kumar, L.M. Ericson, R.H. Hauge, R.E. Smalley, Crystallization and orientation studies in polypropylene/single wall carbon nanotube composite, Polymer, Vol. 44, No. 8, 2003, pp. 2373-2377, DOI: 10.1016/S0032-3861(03)00073-9

[27] A. Patti, P. Russo, D. Acierno, S. Acierno, The effect of filler functionalization on dispersion and thermal conductivity of polypropylene/multi wall carbon nanotubes composites, Composites Part B: Engineering, Vol. 94, 2016, pp. 350-359, DOI: 10.1016/j.compositesb.2016.03.072

[28] V. Patel, U. Joshi, A. Joshi, B.K. Matanda, K. Chauhan, A.D. Oza, D.-P. Burduhos-Nergis, D.-D. Burduhos-Nergis, Multi-walled carbon-nanotube-reinforced PMMA nanocomposites: An experimental study of their friction and wear properties, Polymers, Vol. 15, No. 13, 2023, Paper 2785, DOI: 10.3390/polym15132785

[29] R. Ashok Gandhi, K. Palanikumar, B.K. Ragunath, J.P. Davim, Role of carbon nanotubes (CNTs) in

improving wear properties of polypropylene (PP) in dry sliding condition, Materials & Design, Vol. 48, 2013, pp. 52-57, DOI: 10.1016/j.matdes.2012.08.081

[30] A. Johnney Mertens, S. Senthilvelan, Abrasive wear performance of CNT/PP composites, Applied Mechanics and Materials, Vol. 592-594, 2014, pp. 1262-1266, DOI: 10.4028/www.scientific.net/AMM.592-594.1262

[31] B.K. Goriparthi, P.N.E. Naveen, H. Ravi Sankar, S. Ghosh, Effect of functionalization and concentration of carbon nanotubes on mechanical, wear and fatigue behaviours of polyoxymethylene/carbon nanotube nanocomposites, Bulletin of Materials Science, Vol. 42, No. 3, 2019, Paper 98, DOI: 10.1007/s12034-019-1746-z

[32] S. Paul, K.S. Choi, D.J. Lee, P. Sudhagar, Y.S. Kang, Factors affecting the performance of supercapacitors assembled with polypyrrole/multi-walled carbon nanotube composite electrodes, Electrochimica Acta, Vol. 78, 2012, pp. 649-655, DOI: 10.1016/j.electacta.2012.06.088

[33] E. Assouline, A. Lustiger, A.H. Barber, C.A. Cooper, E. Klein, E. Wachtel, H.D. Wagner, Nucleation ability of multiwall carbon nanotubes in polypropylene composites, Journal of Polymer Science Part B: Polymer Physics, Vol. 41, No. 5, 2003, pp. 520-527, DOI: 10.1002/polb.10394

[34] W. Leelapornpisit, M.-T. Ton-That, F. Perrin-Sarazin, K.C. Cole, J. Denault, B. Simard, Effect of carbon nanotubes on the crystallization and properties of polypropylene, Journal of Polymer Science Part B: Polymer Physics, Vol. 43, No. 18, 2005, pp. 2445-2453, DOI: 10.1002/polb.20527

[35] D.G. Papageorgiou, K. Chrissafis, D.N. Bikiaris, β-nucleated polypropylene: Processing, properties and nanocomposites, Polymer Reviews, Vol. 55, No. 4, 2015, pp. 596-629, DOI: 10.1080/15583724.2015.1019136

[36] D.G. Papageorgiou, G.Z. Papageorgiou, E. Zhuravlev, D. Bikiaris, C. Schick, K. Chrissafis, Competitive crystallization of a propylene/ethylene random copolymer filled with a β-nucleating agent and multi-walled carbon nanotubes. Conventional and ultrafast DSC study, The Journal of Physical Chemistry B, Vol. 117, No. 47, 2013, pp. 14875-14884, DOI: 10.1021/jp409395h

[37] P. Liu, Modifications of carbon nanotubes with polymers, European Polymer Journal, Vol. 41, No. 11, 2005, pp. 2693-2703, DOI: 10.1016/j.eurpolymj.2005.05.017

[38] N.D. Aparna, P. Tambe, Boron nitride nanosheets and silica nanoparticles reinforced polypropylene: Rheological, thermal, mechanical and tribological behaviour, Tribology and Materials, Vol. 4, No. 1, 2025, pp. 18-28, DOI: 10.46793/tribomat.2025.002